Journal of Process Control xxx (2018) xxx–xxx

Contents lists available at ScienceDirect

Journal of Process Control

journal homepage: www.elsevier.com/locate/jprocont

Real-time energy management for electric arc furnace operation☆

Smriti Shyamal, Christopher L.E. Swartz*

Department of Chemical Engineering, McMaster University, 1280 Main St W, Hamilton, ON L8S 4L7, Canada

ARTICLE INFO

Article history:
Received 15 April 2017
Received in revised form 14 February 2018
Accepted 4 March 2018
Available online xxx

Keywords:
Energy management
Electric arc furnace
Moving horizon estimation
Economic model predictive control
Initialization

ABSTRACT

Electric arc furnaces are used extensively in the steel industry for steel production. Development of energy savings strategies for the highly energy-intensive batch process is extremely challenging due to the complexity of the process and lack of measurements due to the harsh operating conditions. Here we introduce a new energy management approach that effectively curtails the energy cost in real-time through the implementation of economically optimal operating decisions. An economics- oriented shrinking horizon nonlinear model predictive control (NMPC) algorithm that exploits time-varying electricity prices is coupled with a multi-rate moving horizon estimator (MHE) to form an integrated decision- making framework. With a detailed first-principles dynamic model functioning at the core, the multi-variable interactions and plant variations are successfully incorporated into the control strategy to achieve reliable performance. We also present a novel initialization scheme for obtaining fast on-line solutions of the economic NMPC and multi-rate MHE dynamic optimization problems. Using this initialization algorithm, we show that the optimal input decisions are obtained with sufficient computational speed for real-time implementation. The energy usage optimization results indicate a significant reduction in the operating cost and peak electricity demand compared to the case where the electricity price profile is not updated.

1. Introduction

Electric arc furnaces (EAFs) are widely used to produce steel by melting down recycled scrap steel. EAF steelmaking contributes more than 25% of the world's total crude steel production [1]. The highly energy intensive batch operation consumes approximately 400 kilowatt-hours/ton [2] of steel produced. Electrical power is transferred to solid scrap by multiple electrodes whereas chemical energy is added through the combustion of injected natural gas and oxygen. As the batch (heat) progresses, the scrap steel melts and forms a flat bath of molten steel at the bottom of furnace. The metal also reacts with oxygen present to give metal oxides which float on top of the molten metal as slag. During the heat, reactions occurring in the slag are controlled by oxygen and carbon lancing, and with some direct lime, carbon and dolomite additions. EAFs have limited measurements due to the harsh operating conditions, with low levels of automation, and rely heavily on the operator's involvement in the decision making process. Although operator's experience is crucial for EAF operation, the complexity of interactions poses a challenge for consistent and optimal operation. Advanced EAF control and optimization strategies can take advantage of more complex relationships to find a cost optimal balance of the energy contributions from chemical reactions and electrical power. The implementation of such an energy management procedure is envisaged to result in significant savings through an optimal utilization of electrical power, natural gas, oxygen, carbon and fluxes such as limestone and dolomite in response to electricity price change.

Electrical energy fulfills approximately 60% of an EAF's total energy requirement [2] . The high dependence on modern power grids to provide the required electricity presents a challenging problem in developing efficient energy management strategies in response to external variations. Power grid operation has recently shifted from a centralized electricity provider to a deregulated approach [3]. Deregulation of electricity allows a competitive market and active consumer participation. Wholesale electricity markets in North America [3–5] generally provide either or all of the following time varying electricity price policies for consumers: day-ahead market (DAM) with price changing every 1-hour, fifteen minute market (FMM), and real-time dispatch (RTD) market with a change every 5- minutes or 1-hour. Electricity cost depends on the time of use and thus there is a high economic incentive for industries to adjust their energy demand according to the volatile market. Companies shifting their high electricity consuming operations from on-peak times to non-peak times of electricity price are generating considerable savings [4] . Another part of the electricity bill is due to the coincidence peak (CP) pricing. Depending

☆ This work is supported by the McMaster Steel Research Center (SRC) and the McMaster Advanced Control Consortium (MACC).
* Corresponding author.
E-mail address: swartzc@mcmaster.ca (C.L.E. Swartz).

https://doi.org/10.1016/j.jprocont.2018.03.002
0959-1524/

on the company's demand contribution in the top specified number of demand peaks over a certain time period (generally 1 year or 4 months), the company is proportionally charged. Thus, there is a great incentive for large-scale consumers to watch for peak demand occurrences and avoid using electricity during the peak time duration. Additionally, such smart plant operation reduces the overall burden on the energy generation side by keeping the real time demand stable with fewer and lower load peaks. A comprehensive real-time energy management strategy with demand response (DR) as a major component within it can be an excellent tool for energy management of EAFs.

Complex industrial facilities typically have a hierarchical decision making structure to compensate for disturbances across multiple time scales and maximize process performance. The hierarchy is composed of planning, scheduling, real-time optimization (RTO), multi- variable control and single-loop regulatory control layers, or a subset thereof. The challenge is to make use of the time-varying electricity price information in all the layers to improve profit. Research efforts directed towards incorporating electricity demand side management into planning and scheduling layers have made significant progress [6]. Low order dynamic models can also be integrated into the scheduling decision making to take advantage of the fast-changing electricity price [7]. Reported research on economic based control of EAFs, suitable for DR operation, is sparse. Control strategies for handling the EAF electrode system have been proposed [8–12], with linear MPC for off-gas control reported in [13,14]. It is only recently that NMPC was proposed using a detailed first principles model of the EAF process [15]. However, full state measurement was assumed and a sequential approach for dynamic optimization was used.

Replacement of the traditional set-point tracking objective in MPC with an economic objective is at the core of recently advanced economic MPC (EMPC) schemes [16,17]. Time varying stage costs have been considered in [18,19], and provide a straightforward way to incorporate a real-time electricity price profile in an economic NMPC formulation. Economic MPC applications considering real-time electricity pricing for continuous processes such as air conditioning (HVAC) systems [20] and a chemical processing plant [21], have been shown to save energy costs. A key potential bottleneck with an EMPC and MHE implementation is the on-line computational demand associated with solving the large scale dynamic optimization problems. Tracking a fast changing electricity price profile and utilizing it to build an energy savings plan requires strategies to avoid the computational delays. To obtain rapid solutions close to the optimal solution, Zavala and Biegler [22] proposed an advanced-step NMPC algorithm based on nonlinear programming (NLP) sensitivity. Real-time algorithms proposed in [23,24] perform a single iteration of the control optimization problem by solving a quadratic programming (QP) problem constructed using the solution of the QP solved at the previous sampling instant. A continuation/generalized minimum residual (GMRES) based method is presented in [25] where a single Newton iteration is performed at each time step to get quick solutions of the optimal control problems. More detailed reviews on real-time algorithms for MHE and NMPC are presented in [26,27]. On the other hand, to obtain optimal solutions online quickly, various on-line initialization strategies are suggested in [26], including shift initialization and initialization based on parametric sensitivities.

In this paper, we aim to develop a real- time energy management strategy for EAF operation. We begin by employing multi-rate MHE to reconstruct the state vector at any point in the batch duration. Although various state estimation tools exist [28,29], MHE has become popular over the past decade [30] because of its constraint handling ability and the use of computationally efficient optimization algorithms. A parameter estimation based multi-rate MHE strategy for EAF operation was presented in an earlier contribution [31]. It used the sequential dynamic optimization approach and the case study showing the MHE tracking ability was for a short simulation horizon. The MHE application was extended in [32] for the full batch time with the use of a simultaneous solution approach to reduce solution time for potential real- time application. However, the MHE in [31,32] was not employed in a closed-loop control application. Although an economic model predictive control was implemented in [33] to deal with multi-rate nature of EAF measurements, it was based on a data-driven dynamic model as opposed to a nonlinear first-principles model as utilized in the present study. A non-time varying NMPC cost function was employed in the EAF application in [15], but perfect state information was assumed, and a sequential optimization approach applied. In the present work, we combine MHE and shrinking horizon EMPC with time varying cost coefficients into a single real-time energy management framework, utilizing a nonlinear first-principles based EAF model. We cast the NMPC and MHE optimization problems as NLP problems using the simultaneous approach to compute optimal solutions for the state estimates and control actions. Additionally, a novel initialization scheme is introduced for a combined MHE-NMPC implementation to obtain rapid solutions. Finally, the efficacy of the proposed energy demand- curbing strategy is demonstrated under RTD electricity pricing scenarios. We also compare the energy savings obtained with and without a price update.

The remainder of the paper is structured as follows: Section 2 describes the first-principles based dynamic EAF model. In Section 3, we present the multi-rate MHE and shrinking horizon economics-based NMPC formulations, as well as the new initialization scheme. Section 4 describes the case studies with results and discussion. Section 5 presents conclusions and identifies future research directions.

2. Electric arc furnace model

The current state of fundamental understanding about the EAF process remains incomplete due to its complexity and extreme operating conditions. The models built using computational fluid dynamics (CFD) [34] to capture details of only a section of furnace are well suited for design and engineering analysis, but are inappropriate for real-time control applications due to long simulation times [35]. Other models developed in the past to simulate an industrial EAF process using simplifying assumptions have focused on partitioning the furnace in multiple zones [36–38]. The heat and mass transfer taking place inside the zones and between the zones is then described using appropriate mathematical equations. The dynamic EAF model proposed in [39] considered 4 equilibrium zones with mass transport limitations (Fig. 1): gas, slag-metal

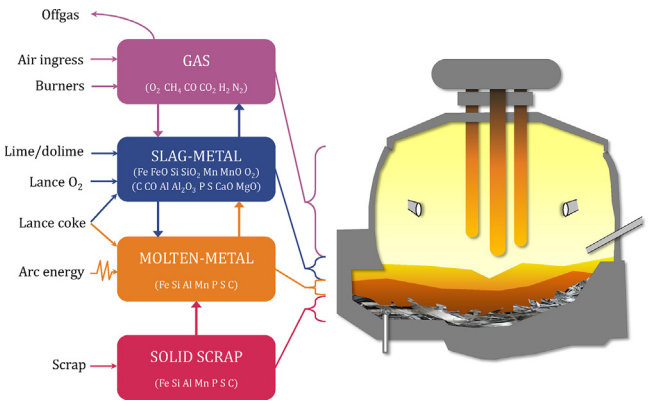

Fig. 1. Schematic of the EAF model [39] employed showing inputs, outputs and material flow between the four zones.

Please cite this article in press as: S. Shyamal, C.L.E. Swartz, Real-time energy management for electric arc furnace operation, J. Process Control (2018), https://doi.org/10.1016/j.jprocont.2018.03.002

interaction, molten steel and solid scrap zones. The *gas zone* contains all the gases filling up the free-board volume of furnace above the scrap steel. Burners are used to preheat the scrap before a high voltage is selected for the arc. The *slag-metal interaction zone* represents all the slag materials in addition to the upper part of molten metal that is in contact with the slag. The *molten steel zone* includes the metals in their liquid form once the scrap starts melting, excluding the portion already considered in the slag-metal interaction zone. The *solid scrap zone* comprises the scrap steel remaining in solid form. To explain the process phenomena in each zone, energy and material balances are considered. A major benefit of using this approach is that it requires fewer parameters than a model based on reaction kinetics. In this paper we employ a modified version of the model developed in [39] to predict the composition and temperature of scrap steel, molten metal, slag and off-gas, as well as slag foam height and its effect on energy transfer from the arc. The model assumes that chemical equilibrium exists in the slag-metal interaction and the gas zones; it computes the chemical equilibrium in each zone by minimization of the Gibbs free energy. Empirical relationships describe the formation of slag foam due to carbon monoxide formation. Atom balances and fundamental mass transfer equations are applied to track the material in each zone and between the zones. The electric arc energy transfer, heat transfer via radiation, chemical reactions and convective heat transfer are taken into account by detailed relationships. MacRosty and Swartz [39] utilized industrial data in a parameter estimation technique based on the maximum likelihood function implemented within gPROMS/gEST [40] to estimate a set of model parameters. The first principles model of [39] was re- calibrated and modified in [41], with two changes incorporated to meet the demands of an another industrial partner. First, a flat surface was assumed for solid scrap melting instead of a cone- frustum geometry, and second, the addition of Jet-Boxes used in the oxygen injection system of the furnace was included. The DAE system coded in the commercial modeling platform gPROMS [40] consisted of 40 differential and 1050 algebraic variables.

The nonlinearities contained in the radiation model of [41] were removed in [31,32] through introduction of a new parameter which affects how energy from the arc power is divided between the furnace roof, walls, the solid scrap and the molten metal. The model parameters were re-tuned to obtain matching profiles for the plant and model data. Since metal oxides were found to be present in trace amounts in the molten metal zone, it was assumed that all the oxides are present in the slag-metal zone only. As a consequence, the corresponding states were eliminated, reducing number of differential states to 29 in the modified model. The gPROMS model is translated to an open-source Python based CasADi [42] framework for application of a simultaneous optimization strategy. State variables of the converted model that attain only small values ($\sim 1.0 \times 10^{-13}$) are removed and replaced with a constant.

Large-scale models pose computational challenges for real-time applications and necessary steps are needed to build a numerically well-behaved DAE system. Our implementation involves a model contraction technique for elimination of a subset of the algebraic variables and equations, using a functionality of CasADi. The CasADi function reformulates the model symbolically by transforming selected algebraic variables into dependent variables, which are determined by explicit expressions involving the differential and retained algebraic variables. The dynamic model employed for this study was consequently contracted to 28 differential and 121 algebraic variables.

3. Formulation and solution strategy

In this section, we describe the proposed real-time energy management strategy for the electric arc furnace operation. A key feature of the strategy involves a model-based real-time optimization implementation wherein an advanced control algorithm provides optimal inputs to the furnace as shown in Fig. 2. Given the real-time electricity price profile $c_{1i}(t)$ and the estimated states $\mathbf{x}_i$ obtained from the moving horizon estimation, the shrinking horizon EMPC finds the optimal inputs $\mathbf{u}_i$. Only the inputs corresponding to the first control stage are injected to the plant. They are also stored for later use in defining the subsequent MHE problems. Once measurements $\mathbf{y}_{i+1}$ are received by MHE, the next set of states is reconstructed. The cyclic strategy continues until the batch ends.

The recursive optimization procedure is computationally demanding. We employ the simultaneous full-discretization approach, in which the input trajectories are parameterized via piecewise constant functions, with an implicit Euler scheme used for the numerical solution of the DAE system. The DAE-constrained optimization problem is thus transformed to a general NLP (nonlinear programming) problem in an entirely algebraic form. Fast solutions of the sparse problem are obtained through the use of an interior-point solver and initialization of the primal and dual variables. The optimal control problems are efficiently initialized by finding good warm-start points using a novel scheme which primarily involves solving background problems in between the sampling time instants. In the subsequent subsections, we present a detailed description of the formulation and solution strategy.

3.1. Shrinking horizon economic model predictive control

MPC formulations based on nonlinear dynamic plant models are typically used for highly nonlinear systems and/or processes that traverse a wide operating range; characteristics generally exhibited in batch operations. Since batch processes have a defined end point, a shrinking horizon formulation where both prediction and control horizons decrease as the controller advances along the batch time is practically desirable [43]. The shrinking hori-

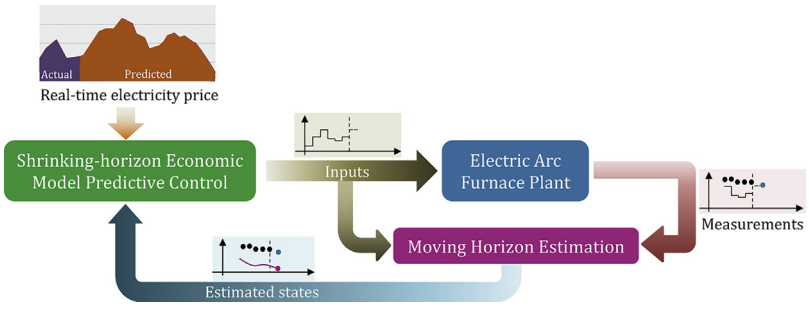

Fig. 2. Real-time energy management control framework.

Please cite this article in press as: S. Shyamal, C.L.E. Swartz, Real-time energy management for electric arc furnace operation, J. Process Control (2018), https://doi.org/10.1016/j.jprocont.2018.03.002

zon economic objective function used for the EAF maximizes the profit opportunity with respect to a single batch operation. Current and predicted energy price trajectories are stitched together to get time-dependent economic NMPC cost coefficients for electric arc power use. It would be ideal to incorporate the model used by wholesale markets for price prediction in the economic NMPC framework since the forecasts are dependent on predicted demand. However, such a model is not easily available and also the expected increase in the NMPC problem dimension might make the on-line implementation infeasible. We assume the price determining mechanism to be independent from the EAF control framework. The price profile is updated every 5, 15 or 60 min depending on the time scale of energy transactions in the market and time when the batch process started. We further assume a deterministic optimization formulation where the forecast is perfectly known without any uncertainty. More sophisticated stochastic formulations where economic NMPC can differentiate between actual and predicted prices are also possible. Apart from the power input, the objective function is time-invariant with respect to the cost of material inputs.

Once the state estimates are obtained from multi-rate MHE (described in the next subsection) a shrinking horizon control problem, with t_f being the fixed end time of the batch, is constructed such that input bounds are satisfied. The DAE system (2) and (3) transformed into algebraic equations upon discretization of the state and control variables, appears as equality constraints. The economic NMPC problem at the current sampling time t_i is given as,

$$\max_{\mathbf{u}(t)} c_0 M_{\text{steel}}(t_f) - \left(\int_{t_i}^{t_f} c_{1i}(t)\text{Pdt} + c_2 \int_{t_i}^{t_f} F_{\text{CH}_4,\text{brnr}}\text{dt} + c_3 \int_{t_i}^{t_f} (Fo_{2,\text{Jetbox1}} + Fo_{2,\text{Jetbox2}} + Fo_{2,\text{Jetbox3}})\text{dt} \right) \quad (1)$$

subject to

Model equations:

$$\dot{\mathbf{x}}(t) = \mathbf{f}(\mathbf{x}(t), \mathbf{z}(t), \mathbf{u}(t)) \quad (2)$$

$$0 = \mathrm{g}(\mathbf{x}(t), \mathbf{z}(t), \mathbf{u}(t)) \quad (3)$$

$$\mathbf{y}(t) = \mathbf{h}(\mathbf{x}(t), \mathbf{z}(t)) \quad (4)$$

$$\mathbf{x}(t_i) = \mathbf{x}_{0i} \quad (5)$$

$$t \in [t_i, t_f] \quad (6)$$

Input constraints:

$$P^{\min}(t) \le P \le P^{\max}(t) \quad (7)$$

$$F_k^{\min}(t) \le F_k \le F_k^{\max}(t). \quad (8)$$

Here P is the active arc power and the natural gas flow rate from the burner is $F_{CH_4,brnr}$. The flow rates of oxygen from the jetboxes 1, 2, and 3 are denoted by $F_{O_2,Jetbox1}$, $F_{O_2,Jetbox2}$, and $F_{O_2,Jetbox3}$ respectively. The amount of molten steel that remains when the batch ends is indicated by M_{steel}. M_{steel} is a state variable. The unit cost associated with each of the control inputs are represented as c_k (k=0, 1, 2, 3). The subscript i in c_1 is used to indicate the time index, thus distinguishing one cost profile from the next. The decision variables for the dynamic optimization problem $\mathbf{u}(t)$ comprise P, $F_{CH_4,brnr}$, $F_{O_2,Jetbox1}$, $F_{O_2,Jetbox2}$, and $F_{O_2,Jetbox3}$. $\mathbf{u}(t)$ is discretized to give piecewise constant controls. The four gas flow rates are denoted in (8) as F_k. The differential and algebraic states of the EAF model are denoted as $\mathbf{x}$ and $\mathbf{z}$ respectively, and the measured outputs as $\mathbf{y}$. $\mathbf{f}$ and $\mathbf{g}$ represent the differential and algebraic functions of the differential- algebraic equation EAF model in semi-explicit form, while $\mathbf{h}$ is a function mapping $\mathbf{x}$ and $\mathbf{z}$ to the measurements $\mathbf{y}$. $\mathbf{x}_{0i}$ denotes the initial condition of the state variables at t_i. The input constraints (7) and (8) provide bounds for each control stage. The added arc power and the gas flows are permitted to move between the upper ($P^{\max}$, $F_k^{\max}$) and lower bounds ($P^{\min}$, $F_k^{\min}$) so that the additions are within realistic limits. The optimal inputs corresponding to the first control stage are implemented on the plant.

3.2. Multi-rate moving horizon estimation

The operation of the EAF is complex, and significant fluctuations occur due to materials being added at multiple time instants during the batch. As the first principles EAF model represents an approximation of the real process phenomenon, plant-model mismatch is likely to exist. Unknown disturbances during the heat can also affect the estimation accuracy and control performance. The state estimation strategy described here handles the uncertainties by employing process noise terms. MHE is well suited for nonlinear constrained estimation because it solves a nonlinear dynamic optimization problem where user-defined constraints are handled directly [44–46]. The use of a fixed estimation horizon in MHE keeps the optimization problem tractable. The MHE implementation typically involves the application of state-of-the art NLP solvers to compute quick solutions in real-time [31,47–49] . The estimation results depend on the availability of plant measurements. This issue arises for EAFs due to a limited number of measurements available for reconstruction of the state vector. Moreover, the measurements are usually taken at different sampling rates. Using all the measurements for estimation potentially improves the system observability which in turn decreases the estimation errors [50,51]. Since MHE uses a past window of measurements it is straightforward to include measurements with variable sampling rate [31,50–53] . The multi-rate formulation described in our earlier work [31] is adopted in the present energy management strategy to take advantage of both the infrequent and frequent measurements.

We consider the EAF process positioned at time instant t_i where i represent the current sampling index, with a past history of measurements and control inputs available. The moving horizon measurement window is of length N control stages. The multi-rate MHE problem formulation considers measurements taken at multiple sampling rates. The infrequent measurements for the EAF are associated with the molten-metal and slag zones, while the frequent measurements correspond to the off-gas composition, and the furnace roof and wall temperatures. We assume that the infrequent measurements are instantaneously available and are located at sampling time instants corresponding to the frequent measurements. We denote $\mathbf{y}_k^F$ as the vector of only frequent measurements, and $\mathbf{y}_k^{SF}$ as the vector containing both the frequent and infrequent measurements. The measurement structure in a moving horizon may be represented, for example, as $\mathbf{Y}_i = \{\mathbf{y}_{i-N}^F, \mathbf{y}_{i-N+1}^{SF}, \mathbf{y}_{i-N+2}^F, \ldots, \mathbf{y}_{i-1}^{SF}, \mathbf{y}_i^F\}$; here the measurement vector at time instant t_{i-N+1} comprises both the infrequent and frequent measurements whereas at sampling time t_{i-N} only frequent measurements are available. The sets of sampling times corresponding to the frequent, and combined frequent and infrequent measurements, are denoted as $\mathbb{I}_F$ and $\mathbb{I}_{SF}$ respectively. The example can be altered to accommodate different structures for $\mathbf{Y}_i$. The measurement sequence is updated at the next sampling time by including the new measurement set while dropping the earliest measurements. This restricts the growth of estimation problem size which also reduces the on-line computational burden. However, if the numerical complexity is not an issue then an expanding horizon least-

Please cite this article in press as: S. Shyamal, C.L.E. Swartz, Real-time energy management for electric arc furnace operation, J. Process Control (2018), https://doi.org/10.1016/j.jprocont.2018.03.002

squares estimation may be more appropriate for the batch process.

The multi-rate MHE optimization problem for a discrete-time nonlinear system observable for the state profile is given as:

$$\min_{\mathbf{x}_{i-N},\mathbf{w}_k} \sum_{k=i-N}^{i-1} ||\mathbf{w}_k||^2_{Q^{-1}} + \sum_{\substack{k=i-N \\ k\in\mathbb{I}_F}}^{i} ||\mathbf{v}_k^F||^2_{(R^F)^{-1}} + \sum_{\substack{k=i-N \\ k\in\mathbb{I}_{SF}}}^{i} ||\mathbf{v}_k^{SF}||^2_{(R^{SF})^{-1}} + ||\mathbf{x}_{i-N} - \hat{\mathbf{x}}_{i-N}||^2_{S_i^{-1}} \tag{9}$$

$$\text{s.t.} \quad \mathbf{x}_{k+1} = \mathbf{f}_k(\mathbf{x}_k, \mathbf{u}_k) + \mathbf{w}_k, \quad k = i-N, \ldots, i-1 \tag{10}$$

$$\mathbf{y}_k^F = \mathbf{h}_k^F(\mathbf{x}_k) + \mathbf{v}_k^F, \quad k \in \mathbb{I}_F \tag{11}$$

$$\mathbf{y}_k^{SF} = \mathbf{h}_k^{SF}(\mathbf{x}_k) + \mathbf{v}_k^{SF}, \quad k \in \mathbb{I}_{SF} \tag{12}$$

$$\mathbf{x}^{LB} \le \mathbf{x}_k \le \mathbf{x}^{UB}, \tag{13}$$

$$\mathbf{w}^{LB} \le \mathbf{w}_k \le \mathbf{w}^{UB}. \tag{14}$$

Here $\mathbf{w}_k$ is included to represent the process noise (i.e. the model uncertainty). $\hat{\mathbf{x}}_{i-N}$ is the *a priori* estimate of the state at the starting point of the moving window. Given the states $\mathbf{x}_k$ and the known inputs $\mathbf{u}_k$, $\mathbf{f}_k(\cdot)$ integrates the process model forward over one sample time. The measurement functions $\mathbf{h}_k^F(\cdot)$ and $\mathbf{h}_k^{SF}(\cdot)$ map the state variables $\mathbf{x}_k$ to the measurements $\mathbf{y}_k^F$ and $\mathbf{y}_k^{SF}$ respectively. The measurement noise terms corresponding to $\mathbf{y}_k^F$ and $\mathbf{y}_k^{SF}$ are represented respectively as $\mathbf{v}_k^F$ and $\mathbf{v}_k^{SF}$. Equation (10) represents a discretized form of the DAE process model in which the algebraic states are considered as functions of the differential states and inputs through (3). The covariance matrices of appropriate dimensions for the model noise, measurement noise and for the arrival cost are represented here as Q, R^F, R^{SF} and S_i. The state constraints are provided by the lower bound $\mathbf{x}^{LB}$ and the upper bound $\mathbf{x}^{UB}$. The model noise $\mathbf{w}_k$ is allowed to move between lower and upper bounds of $\mathbf{w}^{LB}$ and $\mathbf{w}^{UB}$ respectively. The estimate of current states $\mathbf{x}_i$ are obtained from the solution of optimization problem stated above.

The least-squares objective function of the multi-rate MHE scheme (9) comprises four terms. The first three terms are a weighted minimization of model and measurement errors over a moving time horizon of length N. The fourth term in (9) is the arrival cost that represents the measurement information not included in the moving window. The covariance S_i is generally updated when the next MHE problem is formulated, to S_{i+1} using the current solution. However, the covariance update is not necessary when the system is strongly observable [46]. An extended Kalman filter covariance propagation equation is commonly used [45],

$$S_{i+1} = Q + A_i[S_i - S_i C_i^T (R + C_i S_i C_i^T)^{-1} C_i S_i] A_i^{-1} \tag{15}$$

where A_i and C_i are matrices in the linearized model,

$$\begin{aligned} \mathbf{x}_{i+1} &= A_i \mathbf{x}_i + B_i \mathbf{u}_i \\ \mathbf{y}_i &= C_i \mathbf{x}_i + D_i \mathbf{u}_i. \end{aligned} \tag{16}$$

We have suppressed the superscripts '*F*' and '*SF*' for R and $\mathbf{y}$ in (15) for ease of readability. However, appropriate dimensions for R and correct measurement functions ($\mathbf{h}_k^F(\cdot)$ or $\mathbf{h}_k^{SF}(\cdot)$) are to be considered when carrying out EKF update (15). The solutions of the current MHE optimization problem (9) are represented as $\mathbf{x}_{i-N}^*$ and $\mathbf{w}_{i-N}^*$. The covariance S_{i+1} can be computed using other filters as well, such as the unscented Kalman filter [54] and constrained particle filter [55]. Note that for time steps t_i with $i \le N$, new measurements are added to the past history in consideration without dropping the oldest one, and also the initial state covariance is not changed.

3.3. Novel initialization scheme for MHE and NMPC

In both MHE and NMPC, subsequent problems are very similar with respect to the input data and problem structure. This important characteristic is utilized by researchers to generate good starting points for the optimization problems [26] . Although the initialization strategies used in the past have been able to reduce the computational time, it is still considered a major bottleneck for on-line control applications [56]. The prior works have focused more on effectively transferring selected and extended information from a previous solve to the next one. On the contrary, strategies for obtaining fast on-line approximate solutions have been shown to work quite well even for complex models [57,58]. Zavala and Biegler [27] utilized the time between sampling times to first solve a predicted NMPC problem and then used sensitivity information to update the predicted solution upon the availability of new measurements. One of the key components of these algorithms that make them so effective is the use of the time between two consecutive sampling instants. In the present work, the idea is utilized in a novel initialization scheme for a coupled MHE-NMPC implementation. The warm-start strategy proposed here generates initialization points very close to the optimal solution of MHE-NMPC. A forward model simulation is executed to obtain predicted measurements for solving predicted MHE-NMPC problems. The predicted MHE-NMPC solutions provide good warm-start points for primal and dual variables of the actual MHE-NMPC problems to be solved based on newly acquired measurements.

Suppose at time instant t_k, we have the following information: the current state estimate $\mathbf{x}_k$ and input $\mathbf{u}_k$. We have suppressed the superscripts used for representing slow and fast measurements for ease of readability. We refer to the time gap between consecutive sampling times of frequent measurements as 'background' time. We introduce an initialization scheme using the given information at time t_k for obtaining fast optimal solutions of MHE-NMPC problems:

In background mode, between t_k and t_{k+1}:

1. Use $\mathbf{x}_k$ and $\mathbf{u}_k$ to generate the predicted future measurements $\bar{\mathbf{y}}_{k+1}$ though a disturbance-free ($\mathbf{w}_k = 0$) model simulation $\bar{\mathbf{x}}_{k+1} = \mathbf{f}(\mathbf{x}_k, \mathbf{u}_k)$ and $\bar{\mathbf{y}}_{k+1} = \mathbf{h}(\bar{\mathbf{x}}_{k+1})$.
2. Construct and solve the predicted MHE problem using $\bar{\mathbf{y}}_{k+1}$ to get predicted state estimates $\bar{\mathbf{x}}_{k+1}$. Retain the problem solution $\tilde{s}_k^{mhe}$ (both primal and dual).
3. Define the predicted NMPC problem using $\bar{\mathbf{x}}_{k+1}$ and the electricity price profile $\bar{c}_{1k}$ known at t_k. Solve the problem to obtain predicted input $\bar{\mathbf{u}}_{k+1}$ and retain the solution $\tilde{s}_k^{nmpc}$ (both primal and dual).

On-line, at t_{k+1}:

1. Receive the *true* measurements $\boldsymbol{y}_{k+1}$ from the plant and solve the *true* MHE optimization problem by employing $\tilde{s}_k^{mhe}$ as initial guesses to compute true state estimates $\mathbf{x}_{k+1}$.
2. Define the *true* NMPC problem using $\mathbf{x}_{k+1}$, and the electricity price profile $c_{1,k+1}$ known at t_{k+1}. Solve the *true* NMPC problem using $\tilde{s}_k^{nmpc}$ as initial guesses to obtain the *true* input $\mathbf{u}_{k+1}$, and return to the background step.

The warm-start scheme can be used with any of the three dynamic optimization approaches: simultaneous, sequential, and multiple shooting (a detailed discussion on the three dynamic optimization approaches is provided in [59]); however, it is particularly useful for the simultaneous approach where initialization of the

Please cite this article in press as: S. Shyamal, C.L.E. Swartz, Real-time energy management for electric arc furnace operation, J. Process Control (2018), https://doi.org/10.1016/j.jprocont.2018.03.002

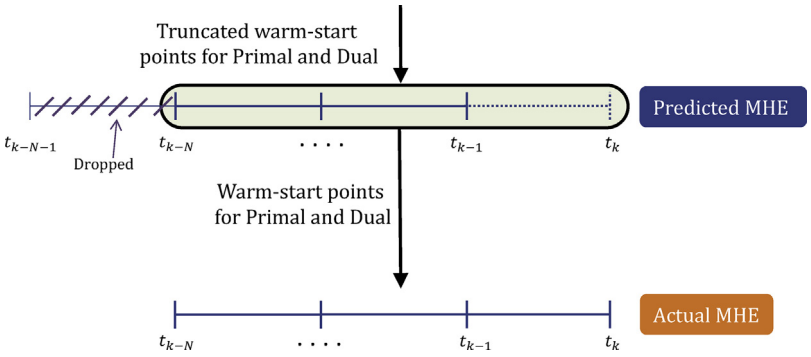

Fig. 3. Initialization for moving horizon estimation.

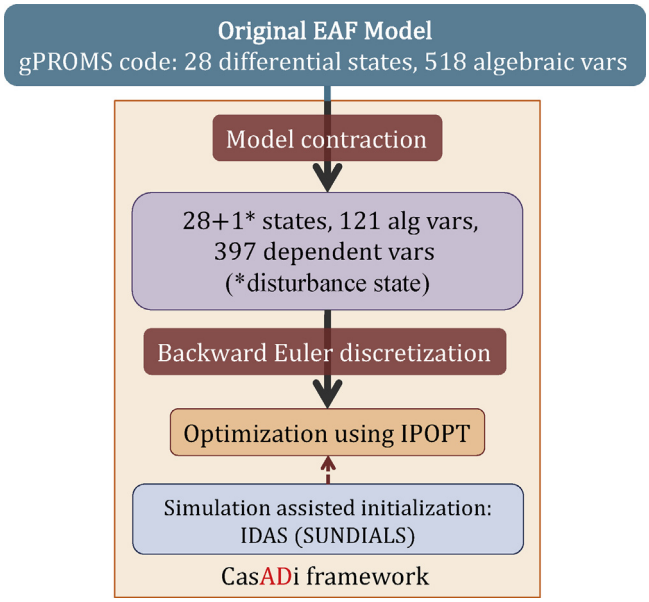

Fig. 4. Dynamic optimization implementation framework.

entire dynamic profiles is required. Depending on the closeness of the predicted and the *true* values, the benefit of the scheme may vary. The initialization is particularly useful for MHE because good warm-start points are consequently available for both the primal and dual variables associated with the new sampling interval of the moving window (Fig. 3). Fig. 3 illustrates how warm-start points are passed from a predicted MHE solve to an actual MHE solve using the proposed initialization scheme.

3.4. Implementation

The energy management strategy is implemented for a discretized model using the Python front end of CasADi. The variable space of the EAF model written in gPROMS is first reduced in CasADi to get a reduced DAE system. Next, the dynamic optimization problems are solved by employing the simultaneous solution approach. We set 7 finite elements per control stage to carry out time discretization for MHE and NMPC. Using the simultaneous approach, the optimal control problems are expressed as large-scale sparse NLP problems, which are then solved with the interior- point solver IPOPT [60] using the linear solver MA27. We employ IDAS (part of the SUNDIALS [61] suite of solvers) for carrying out the plant and model simulations required for the forward integration and measurement generation. To warm-start the predicted MHE and NMPC problems, the primal and the dual information is transferred from their respective last *true* optimization solves. However, the MHE solution set is shortened by removing the first control stage values. The initial guesses for the primal values associated with the new terminal stage are obtained by a forward simulation. For the shrinking horizon NMPC, the variable values are dropped for the first time interval. The *true* MHE-NMPC problems are initialized with the primal and dual values of respective predicted solves. The implementation framework is illustrated in Fig. 4.

To include plant-model mismatch in our implementation, we decrease a power factor parameter k_p by 10% in the model used by MHE and NMPC. Due to the mismatch, the amount of electrical energy delivered to the solid scrap by the arc is decreased significantly within the MHE and NMPC models. The exact model equations affected by a perturbation in k_p is given in [41]. Since unmeasured disturbances can result in unsatisfactory MHE performance, we compensate the mismatch by augmenting the model states with an integrated disturbance state $\mathbf{d}_k$, assumed to be driven only by white noise $\mathbf{w}_{dk}$. MHE is implemented by employing the augmented system

$$\begin{aligned} \mathbf{x}_{k+1} &= \mathbf{f}_k(\mathbf{x}_k, \mathbf{u}_k) + \mathbf{B}_d\mathbf{d}_k + \mathbf{w}_k, \\ \mathbf{y}_k^F &= \mathbf{h}_k^F(\mathbf{x}_k) + \mathbf{v}_k^F, \\ \mathbf{y}_k^{SF} &= \mathbf{h}_k^{SF}(\mathbf{x}_k) + \mathbf{v}_k^{SF}, \\ \mathbf{d}_{k+1} &= \mathbf{d}_k + \mathbf{w}_{dk}, \end{aligned} \tag{17}$$

where $\mathbf{B}_d$ adjusts the impact of disturbance state $\mathbf{d}_k$ on the state equation. $\mathbf{Q}_d$ represents the covariance of $\mathbf{w}_{dk} \sim \mathcal{N}(0, \mathbf{Q}_d)$. Disturbance models are discussed in greater depth in [51] . For the case studies presented in the next section, we have included the disturbance state in the differential equation corresponding to the state variable which represents the moles of manganese in the slag-metal zone. To implement this, we used $\mathrm{B}_d = e_i \in \mathbb{R}^n$ where i represents the state corresponding to the number of moles of manganese in the state vector of size n, and e_i is the ith unit vector. $\mathbf{Q}_d$ is chosen as 0.2 for the case studies described in the next section.

4. Case studies

In this section we present four case studies to demonstrate potential benefits of a real-time implementation of the proposed energy management strategy. The studies correspond to changing electricity prices in a real-time dispatch market (RTD), with the price changing every hour. We also analyze the multi-rate MHE's ability to track the true states. Finally, we discuss the computational effort required to solve the MHE and NMPC dynamic optimization problems.

For testing the on-line energy management strategy, we utilize the first-principles EAF model comprising 28 differential and 121 algebraic states. The batch process is 60 min in duration, during

Please cite this article in press as: S. Shyamal, C.L.E. Swartz, Real-time energy management for electric arc furnace operation, J. Process Control (2018), https://doi.org/10.1016/j.jprocont.2018.03.002

Table 1
Multi-rate measurement structure for the case study.

Time (min)	0 · · · 42	43	44 · · · 46	47	48 · · · 60
Number of measured variables	6	**13**	6	**8**	6

Table 2
Measurement availability in the case study.

Measurement	Sampling time	Variance
Off-gas compositions (CO, CO_2, O_2, H_2) (dimensionless)	Every 1 min	0.01
T_{roof}, T_{wall} (K)	Every 1 min	3
Slag compositions (FeO, Al_2O_3, SiO_2, MgO, CaO)(dimensionless)	43rd min	0.1
Molten-metal temperature (K)	43rd &47th min	5
Molten-metal carbon content (dimensionless)	43rd &47th min	0.01

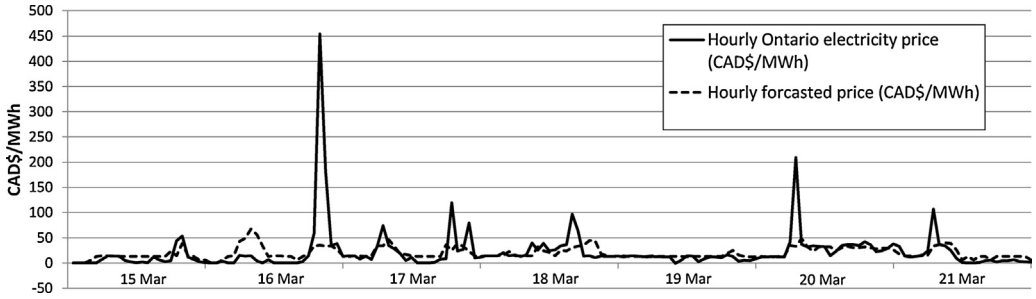

Fig. 5. Hourly Ontario (Canada) electricity price (actual and predicted) for 15–21 March 2017.

which scrap metal is charged at time $t = 0$ and $t = 25$ min. The measurements for the process are available at different sampling rates, shown in Table 1. The frequent measurements are off-gas compositions and furnace roof and wall temperatures with a sampling time of 1 min. Slag chemistry data is available only at the 43rd minute of the heat duration. The molten metal temperature and carbon content are known at the 43rd and 47rd minute. The measurement data and the variance values are summarized in Table 2. With limited availability of frequent measurements, it is important to analyze the observability of the system before state estimation is carried out. This was assessed by computing the observability of the states of the linearized DAE model at each sampling time instant, using the state observability metric defined in [51]. It utilizes the singular value decomposition (SVD) of the observability matrix constructed from matrices A_i and C_i in the state space model (16). Since the lowest metric value obtained was 7.0×10^{-7}, the system is deemed to be fully observable. It is to be noted that the linearization procedure adopted here is not essential because the system observability can also be inferred by examining the IPOPT output [48]. The key step associated with this procedure involves extracting the reduced Hessian information from the IPOPT solution.

4.1. Actual and predicted electricity prices

To make sure that the case studies are conducted using realistic pricing scenarios, we analyzed the actual and predicted hourly electricity prices in the province of Ontario (Canada) for 2016 and the first four months of 2017. Electricity price profiles are generally volatile and high spikes occur rather frequently. Fig. 5 shows the variation in electricity price over 15–21 March 2017. We can observe the price spikes and the inability of the forecast model employed by Ontario IESO (Independent Electricity System Operator) to predict these spikes. Upon studying the hourly price and the predictions for 2016, we observed that the predictions were 87.2% less than actual prices on average when the actual prices were greater than \$200/MWh. The actual prices exceeded \$200/MWh for 19 hourly price durations. The prices were between \$100/MWh and

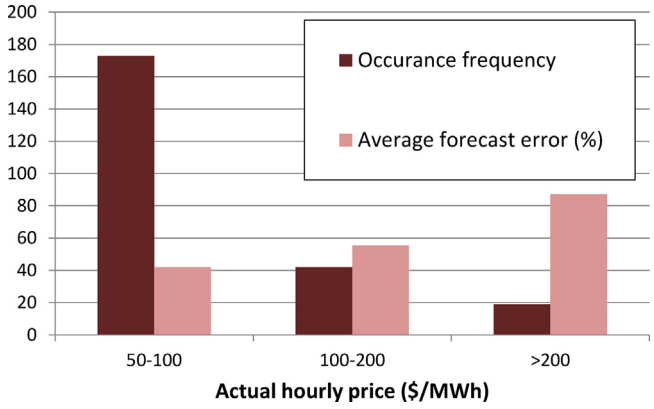

Fig. 6. Price forecast error analysis for 2016 for the Ontario electricity wholesale market.

\$200/MWh in 42 hourly periods, and the average prediction difference was 55.4%. For the price range \$50–\$100/MWh, the occurrence frequency was 173 (14.4 per month on average), with the average forecast error at 42%. The analysis is summarized in Fig. 6. The high magnitude of forecast error motivates us to study the economic impact of electricity price profile updates in the NMPC objective function. The following four case studies demonstrate the NMPC performance when different electricity price trajectories are encountered. The case studies are summarized in Table 3.

4.2. Case study 1: price peak decrease with price change at 25th min

Our first case study quantifies the economic performance of NMPC subject to an electricity price change at time $t = 25$th minute of the batch duration. The electricity price is \$308.24/MWh before the 25th min and \$ 190.48/MWh after the change. The price prediction for 25–60 min at time $t = 0$ min is \$10.96/MWh. The price variation corresponding to this case occurred in the Ontario mar-

Please cite this article in press as: S. Shyamal, C.L.E. Swartz, Real-time energy management for electric arc furnace operation, J. Process Control (2018), https://doi.org/10.1016/j.jprocont.2018.03.002

Table 3
Summary of the case studies comparing NMPC^{nom} with NMPC^{up}. Wherever % is shown, the values are with respect to NMPC^{nom}. The time of electricity price change is the time instant during the batch process of length 60 min.

Case no.	1	2	3	4
Time of electricity price change (min)	25	25	40	15
Electricity price before the change ($/MWh)	308.24	30	308.24	308.24
Electricity price after the change ($/MWh)	190.48	200	190.48	190.48
Predicted electricity price ($/MWh)	10.96	15	10.96	10.96
Economic objective increase (%)	4.62	1.54	3.45	3.48
Decrease in electric power use (%)	23.06	8.49	17.34	17.9
Increase in other input use (%)	1.59	0.68	0.15	4.58
Reduction in peak electricity demand (%)	44.62	10.12	14.15	10.11

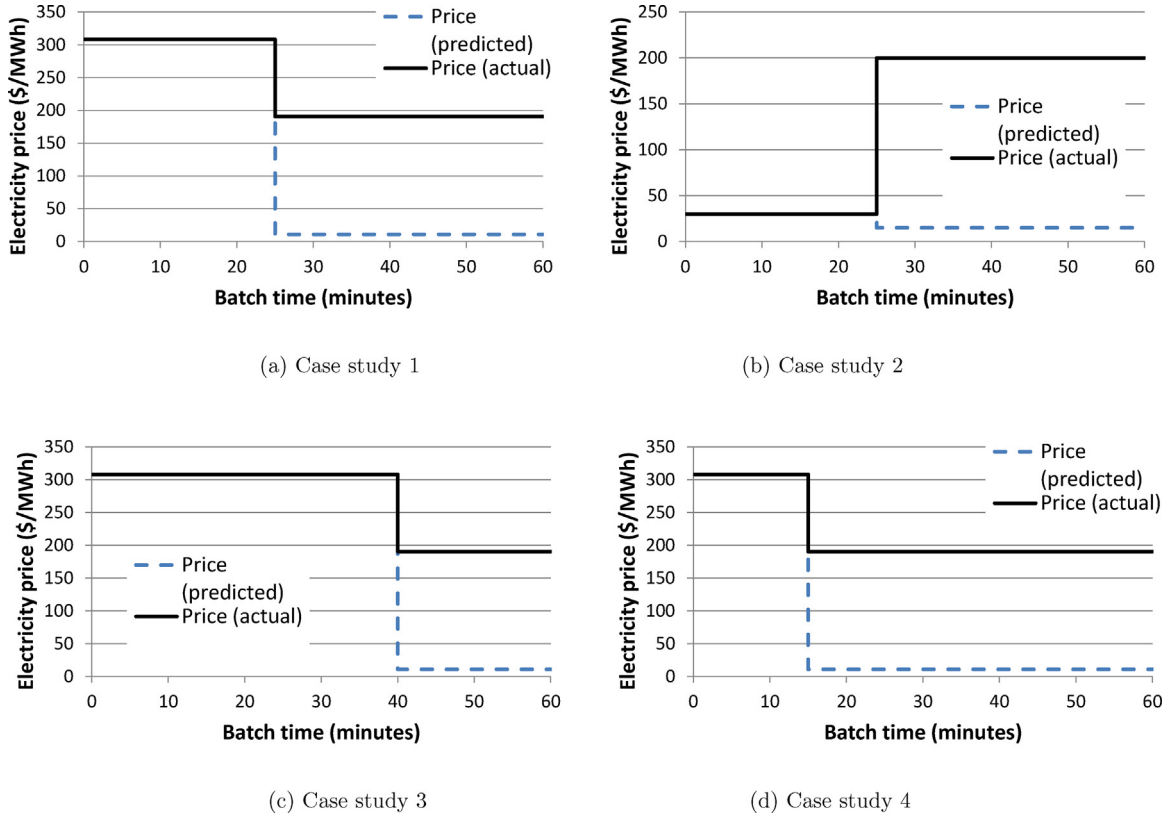

(a) Case study 1 (b) Case study 2

(c) Case study 3 (d) Case study 4

Fig. 7. Electricity price profiles for the four case studies. The electricity price variation is for a 1 h electricity price market.

ket at 21:00–22:00 h (7th April 2017), and is represented in Fig. 7a. The price profile is typical when the batch process is operated during the descent part of an electricity price peak. The price forecast error is expected to be high in such cases.

Here we are comparing two closed loop results, the first (NMPC^{nom}) where the price profile is not updated and the forecast price is continued to be used even after 25th minute, and the second (NMPC^{up}) where the price profile is updated at the 25th minute to reflect the actual price obtained from the wholesale market. We achieve a 4.62% increase in economic objective value when the price profile is updated. The economic objective increase is due to the fact that NMPC^{up} is able to see a higher price than the forecast for electricity post 25th min, and thus uses 23.06% less electrical energy and 1.59% more of the other inputs (CH_4 and O_2). The NMPC^{nom} sees a electricity price profile very different from the actual price post 25th min, and thus is not able to use the control inputs in a cost efficient manner. The normalized input profiles for both NMPC^{nom} and NMPC^{up} are given in Fig. 8. The input profiles are scaled for proprietary reasons. From Fig. 8, it is apparent that NMPC^{nom} uses significantly higher electric arc power after 25th minute. Examining the other input trajectories, it can be seen that the CH_4 input is not showing a major difference but O_2 consumption though the three jetboxes for NMPC^{up} is higher than that of NMPC^{nom}. Although we observe a large decrease in the electrical power use, the economic objective is not increased by that factor because less molten steel is produced when the total energy consumption is lower. Even though peak electricity demand minimization is not specifically formulated in the NMPC objective function, the peak demand for NMPC^{up} is 44.62% less than NMPC^{nom}. Peak shaving is an added advantage of using NMPC^{up} and is important for both the power grid and steel-industry sides. However, a more direct mathematical formulation to minimize peak demand is essential to study the economic trade-offs. The trajectories for off-gas measurements for the plant are shown in Fig. 9. We can notice that CO consumption is more for NMPC^{up}. NMPC^{up} works with the exact price profiles and is thus able to optimally identify CO as an energy source. It uses 0.16% less of CH_4 and instead generates energy though CO combustion. This is useful in economics and also, there is a decreased impact on the environment.

Please cite this article in press as: S. Shyamal, C.L.E. Swartz, Real-time energy management for electric arc furnace operation, J. Process Control (2018), https://doi.org/10.1016/j.jprocont.2018.03.002

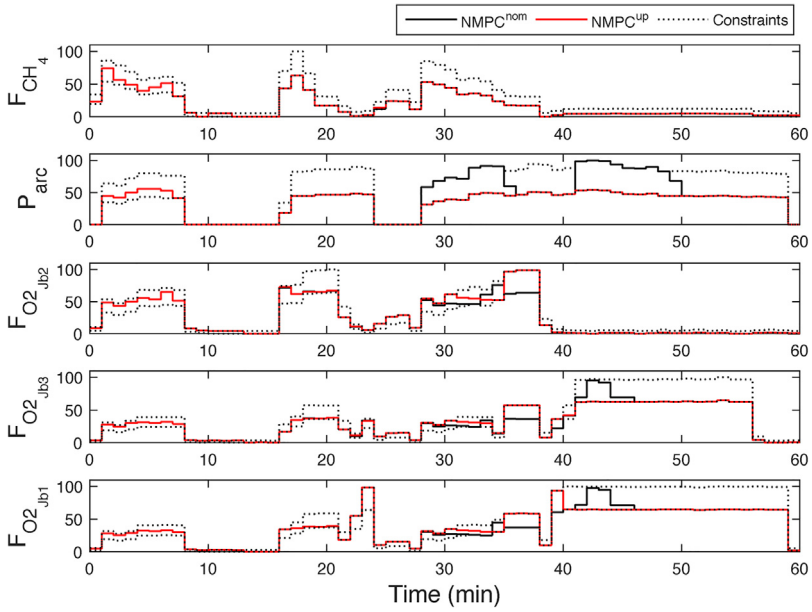

Fig. 8. Case study 1: input variable profiles.

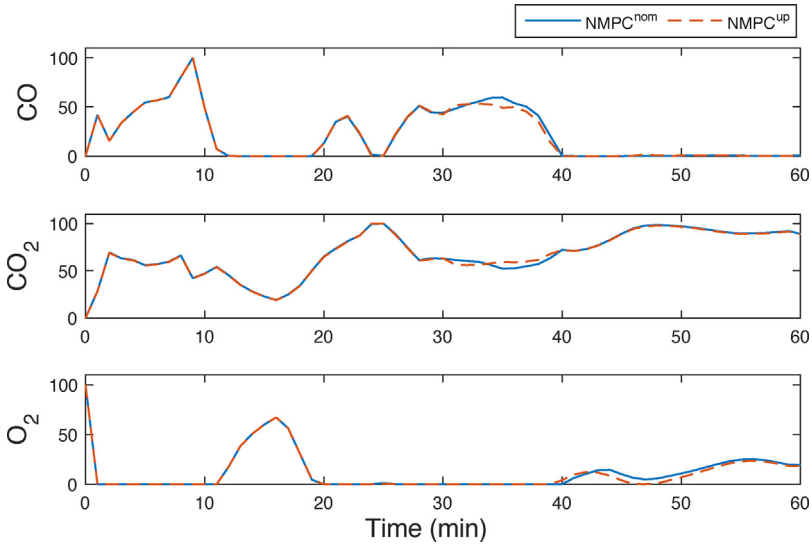

Fig. 9. Case study 1: off-gas profiles, scaled to within their maximum and minimum ranges.

4.3. Case study 2: price peak increase with price change at 25th min

Next, we investigate the effect of an electricity price profile with different characteristics. We again choose the price change time instant as the 25th minute of the batch duration (see Fig. 7b). The actual prices are \$30/MWh and \$200/MWh before and after the change respectively. The predicted price is \$15/MWh as the forecast model is not able to predict a sudden change in the price profile. In this case, NMPC^{up} gives us a 1.54% increase in economic objective value compared to NMPC^{nom}. The increase is lower compared to case study 1 mainly due to the batch operating under a lower actual electricity price (see Fig. 7b). This results in more scrap being melted earlier in the batch through increased arc power (see Fig. 7b), with less opportunity to reduce costs over the remainder of the batch. The electricity consumption for NMPC^{up} is 8.49% less and other inputs are utilized more by 0.68%. The input profiles are shown in Fig. 10. The peak electricity demand during the batch operation is reduced by 10.12% if NMPC^{up} is used instead of NMPC^{nom}.

4.4. Case study 3: price decrease with a price change at 40th min

This case study uses the same electricity price data of case study 1 but a change in electricity price occurs at the 40th minute of the batch time (see Fig. 7c). We obtain a 3.45% increase in economic objective value when NMPC^{up} is employed instead of NMPC^{nom}. The economic objective value increase is less than case study 1 because the forecast error encountered by NMPC^{nom} is for a smaller section of the batch time span. NMPC^{up} utilizes 17.34% less electrical energy and 0.15% more of the other inputs. The peak electricity demand for NMPC^{up} is 14.15% less than that of NMPC^{nom}.

4.5. Case study 4: price decrease with a price change at 15th min

The electricity price data of case study 1 is utilized in this case study, except a change in electricity price occurs at the 15th minute of the batch time (see Fig. 7d). NMPC^{up} continues to give a better economic objective value (3.48% increase) when compared with the NMPC^{nom} implementation. Although a greater economic objective value percent increase may be expected due to the earlier

Please cite this article in press as: S. Shyamal, C.L.E. Swartz, Real-time energy management for electric arc furnace operation, J. Process Control (2018), https://doi.org/10.1016/j.jprocont.2018.03.002

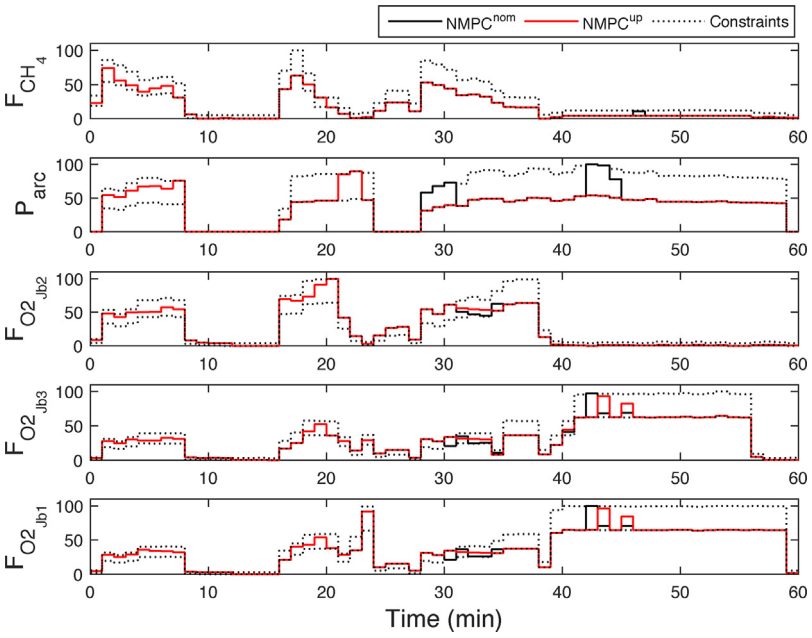

Fig. 10. Case study 2: input variable profiles.

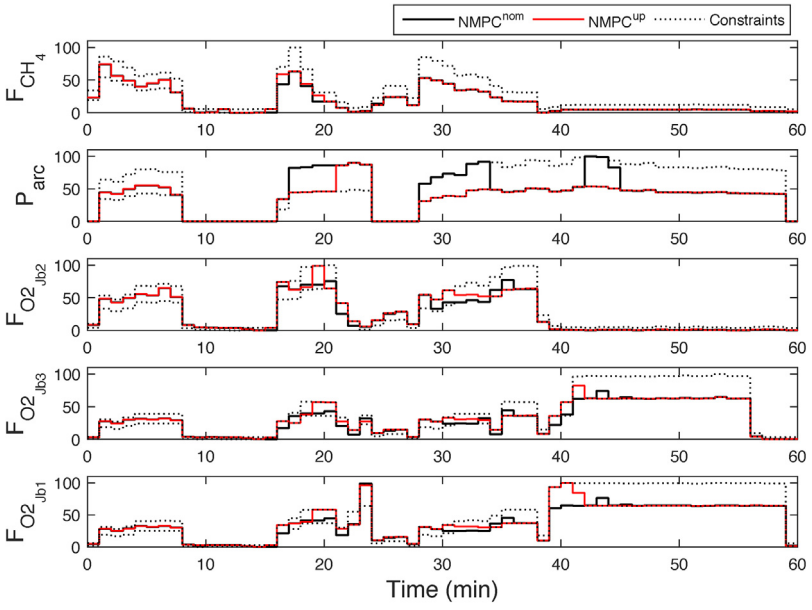

Fig. 11. Case study 4: input variable profiles.

electricity price change, this is offset against the shorter duration of the initial high electricity price ($308/MWh). This results in higher power usage by both schemes before the 25th minute (see Fig. 11) with more scrap being melted during this period and less opportunity for cost reduction for the remainder of the batch. NMPC^{up} consumes 17.9% less electric arc power and 4.58% more for the other inputs relative to NMPC^{nom}. The input profiles are shown in Fig. 11. The peak electricity demand point for NMPC^{up} is lowered by 10.11% in comparison to the maximum electric arc power utilization during the NMPC^{nom} implementation.

4.6. Multi-rate MHE performance

We demonstrate the performance of multi- rate MHE in the presence of initial state discrepancy, plant-model mismatch and measurement noise. In all the case studies, the *true* initial conditions are perturbed by adding Gaussian noise with 1% relative variance. As discussed in Section 3.4, plant- model mismatch is artificially created by decreasing the power factor parameter k_p by 10%. Gaussian measurement noise is added to the *true* measurements according to their respective variances given in Table 2. The covariance matrix Q for model noise is selected based on a detailed analysis of multiple simulations. The moving horizon length is chosen to be 6 min. We also introduced upper and lower bounds for the differential states, the algebraic states, and the model noise variables. A subset of the *true* and estimated state variables is plotted with respect to time for case 1 in Fig. 12. We can observe that the multi- rate MHE is able to track the *true* states with good accuracy despite the multiple sources of error.

4.7. Computational results

An Intel Core i7-3770 processor with 4 CPU cores running Windows 7 at 3.40 GHz was used for all the numerical computations.

Please cite this article in press as: S. Shyamal, C.L.E. Swartz, Real-time energy management for electric arc furnace operation, J. Process Control (2018), https://doi.org/10.1016/j.jprocont.2018.03.002

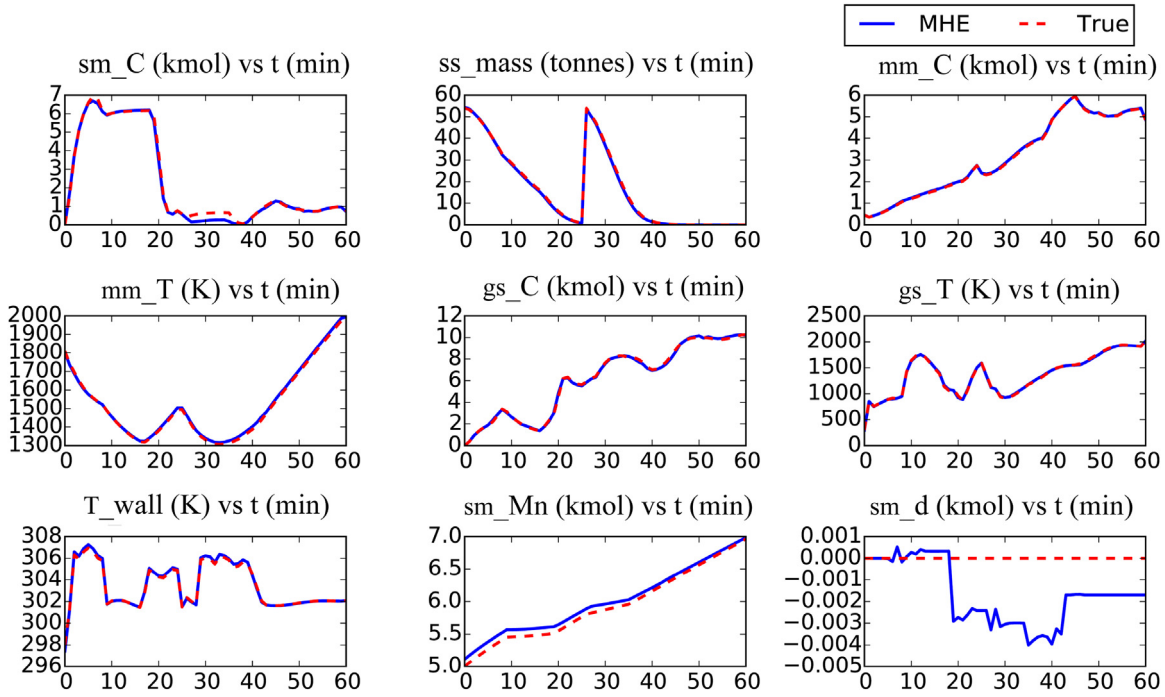

Fig. 12. State estimates for case study 1 with respect to time (in min). sm_C: carbon in slag-metal zone, ss_mass: solid scrap mass, mm_C: carbon in molten metal zone, mm_T: temperature of molten metal, gs_C: carbon in gas zone, gs_T: temperature of gas, T_wall: furnace wall temperature, sm_Mn: manganese in slag-metal zone, sm_d: disturbance state in slag-metal zone.

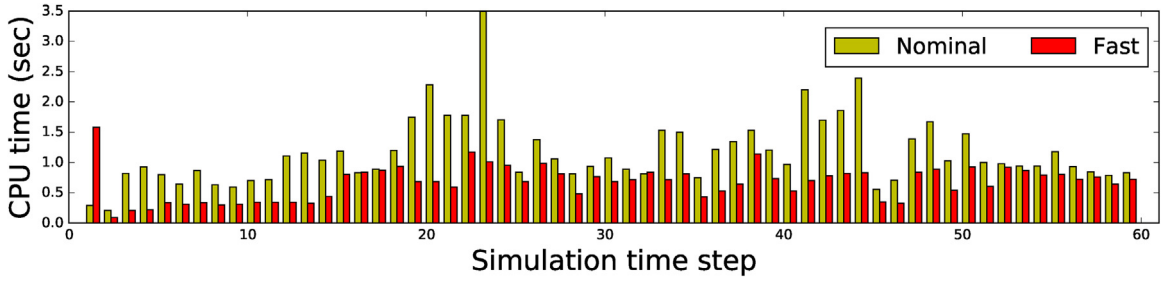

Fig. 13. Solution times for MHE problems with horizons of $N = 6$ time steps. The solve time denoted by 'fast' represents computational time when the proposed initialization scheme is used. 'Nominal' represents the MHE solves carried out without the use of the proposed initialization scheme.

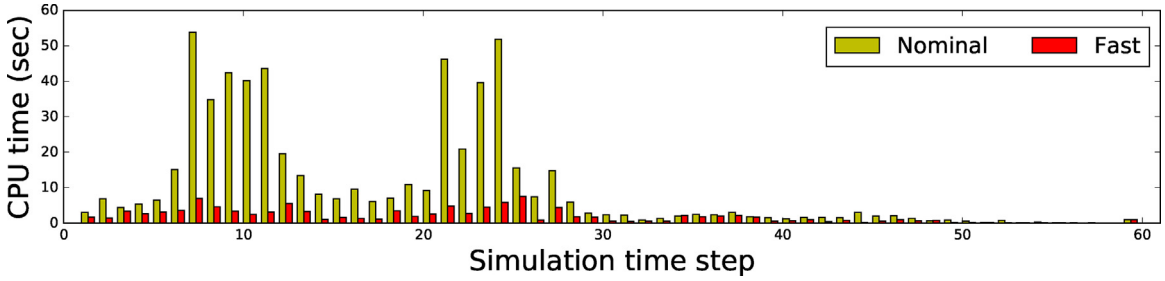

Fig. 14. Solution times for shrinking horizon NMPC problems. The solve time denoted by 'fast' represents computational time when the proposed initialization scheme is used. 'Nominal' represents the NMPC solves carried out without the use of the proposed initialization scheme.

The CPU times required to solve the multi-rate MHE problems for case study 1 (NMPC^{up}), using the proposed initialization (fMHE) and without using the scheme (nMHE), are shown in Fig. 13. The computational results for fNMPC (NMPC using the proposed initialization scheme) and nNMPC (NMPC without using the scheme) are presented in Fig. 14. We observe that the initialization scheme is able to reduce the computation time for both the MHE and NMPC significantly. The average CPU time required to solve the fMHE, nMHE, fNMPC and nNMPC problems are 0.7, 1.2, 1.9 and 10 s respectively. Thus, there is 76.8% decrease in total (MHE + NMPC) on-line CPU solve time when the proposed initialization scheme is used. Furthermore, computational times required for background MHE and NMPC solves are well within 1 min.

5. Conclusions and future work

In this work we developed a real-time energy management strategy for batch operation of electric arc furnaces. The strategy

Please cite this article in press as: S. Shyamal, C.L.E. Swartz, Real-time energy management for electric arc furnace operation, J. Process Control (2018), https://doi.org/10.1016/j.jprocont.2018.03.002

is efficient in reducing the energy requirements while effectively exploiting the changing electricity prices. The optimal inputs are computed with the use of a coupled MHE-NMPC application. Moreover, a novel initialization scheme is proposed to reduce the online solution times for the multi-rate MHE and shrinking horizon economics-based NMPC problems. The scheme uses the time between consecutive sampling times to generate warm start points for the upcoming on-line MHE-NMPC solves.

Our case studies focused on demonstrating NMPC economic performance in multiple scenarios of varying electricity prices. NMPC tackled the price variations by balancing the control inputs used to provide the electrical and chemical energy to the process. The challenging EAF process is operated within realistic limits by the economics-based NMPC. The strong convergence ability shown by the multi-rate MHE provided appropriate estimates to the NMPC. With modern power grids moving towards a smarter operation and generation, the proposed strategy can actively fit into and support this new energy utilization and consumption ecosystem. The case studies showed that the high energy intensive EAFs are capable of aiding the power grid by adjusting its operation in real-time through the use of advanced control tools NMPC and MHE.

Immediate next steps are formulating an NMPC problem that can minimize the peak demand. We also aim to explore NMPC and MHE formulations for the variable batch length problem and incorporate them into an upper level scheduling layer. The integration of scheduling and control is envisaged to generate economic benefit due to better utilization of EAF operating resources. Furthermore, in-plant evaluation of the energy management strategy would be a useful step toward industrial adoption.

References

[1] Steel Statistical Yearbook of World Steel Association, 2016 http://www.worldsteel.org/steel-by- topic/statistics/steel-statistical-yearbook-.html.
[2] R.J. Fruehan, The Making, Shaping, and Treating of Steel: Ironmaking, vol. 2, AISE Steel Foundation, 1999.
[3] A.W. Dowling, R. Kumar, V.M. Zavala, A multi-scale optimization framework for electricity market participation, Appl. Energy 190 (2017) 147–164.
[4] Energy Management Brochure for Businesses by IESO Ontario, 2016 http://www.ieso.ca/-/media/files/ieso/document- library/publications/the-bottom-line-on-energy-management.pdf? la=en.
[5] Q. Wang, C. Zhang, Y. Ding, G. Xydis, J. Wang, J. Østergaard, Review of real-time electricity markets for integrating distributed energy resources and demand response, Appl. Energy 138 (2015) 695–706.
[6] Q. Zhang, I.E. Grossmann, Planning and scheduling for industrial demand side management: advances and challenges, in: Alternative Energy Sources and Technologies, Springer, 2016, pp. 383–414.
[7] R. Pattison, C.R. Touretzky, T. Johansson, M. Baldea, I. Harjunkoski, Moving horizon scheduling of an air separation unit under fast-changing energy prices, IFAC PapersOnLine 49 (7) (2016) 681–686.
[8] S. Billings, F. Boland, H. Nicholson, Electric arc furnace modelling and control, Automatica 15 (2) (1979) 137–148.
[9] A. Morris, M. Sterling, Identification and direct digital control of an electric arc furnace controller, in: IEE Proceedings D (Control Theory and Applications), vol. 128, IET, 1981, pp. 123–128.
[10] R. Nadira, P.B. Usoro, Self-adjusting model algorithmic control of a three-phase electric arc furnace, in: American Control Conference, 1988, IEEE, 1988, pp. 227–232.
[11] P. King, M. Nyman, Modeling and control of an electric arc furnace using a feedforward artificial neural network, J. Appl. Phys. 80 (3) (1996) 1872–1877.
[12] B. Boulet, G. Lalli, M. Ajersch, Modeling and control of an electric arc furnace, in: American Control Conference (ACC), vol. 4, IEEE, 2003, pp. 3060–3064.
[13] D. Oosthuizen, I. Craig, P. Pistorius, Model predictive control of an electric arc furnace off-gas procedure combined with temperature control, in: Africon, vol. 1, IEEE, 1999, pp. 415–420.
[14] J. Bekker, I. Craig, P. Pistorius, Model predictive control of an electric arc furnace off-gas process, Control Eng. Pract. 8 (4) (2000) 445–455.
[15] R.D.M. MacRosty, C.L.E. Swartz, Nonlinear predictive control of an electric arc furnace, IFAC Proc. Vol. 40 (11) (2007) 285–290.
[16] R. Amrit, J.B. Rawlings, D. Angeli, Economic optimization using model predictive control with a terminal cost, Annu. Rev. Control 35 (2) (2011) 178–186.
[17] M. Ellis, H. Durand, P.D. Christofides, A tutorial review of economic model predictive control methods, J. Process Control 24 (8) (2014) 1156–1178.
[18] M. Ellis, P.D. Christofides, Economic model predictive control with time-varying objective function for nonlinear process systems, AIChE J. 60 (2) (2014) 507–519.
[19] D. Angeli, A. Casavola, F. Tedesco, Theoretical advances on economic model predictive control with time-varying costs, Annu. Rev. Control 41 (2016) 218–224.
[20] D.I. Mendoza-Serrano, D.J. Chmielewski, Smart grid coordination in building HVAC systems: EMPC and the impact of forecasting, J. Process Control 24 (8) (2014) 1301–1310.
[21] J. Feng, A. Brown, D. O'Brien, D.J. Chmielewski, Smart grid coordination of a chemical processing plant, Chem. Eng. Sci. 136 (2015) 168–176.
[22] V.M. Zavala, L.T. Biegler, The advanced-step NMPC controller: optimality, stability and robustness, Automatica 45 (1) (2009) 86–93.
[23] M. Diehl, R. Findeisen, F. Allgöwer, H.G. Bock, J.P. Schlöder, Nominal stability of real-time iteration scheme for nonlinear model predictive control, IEE Proc. Control Theory Appl. 152 (3) (2005) 296–308.
[24] D. DeHaan, M. Guay, A new real-time approach for nonlinear model predictive control, IFAC Proc. Vol. 38 (1) (2005) 1007–1012.
[25] T. Ohtsuka, A continuation/GMRES method for fast computation of nonlinear receding horizon control, Automatica 40 (4) (2004) 563–574.
[26] M. Diehl, H.J. Ferreau, N. Haverbeke, Efficient numerical methods for nonlinear MPC and moving horizon estimation, in: Nonlinear Model Predictive Control, Springer, 2009, pp. 391–417.
[27] L. Biegler, X. Yang, G. Fischer, Advances in sensitivity-based nonlinear model predictive control and dynamic real-time optimization, J. Process Control 30 (2015) 104–116.
[28] D. Dochain, State and parameter estimation in chemical and biochemical processes: a tutorial, J. Process Control 13 (8) (2003) 801–818.
[29] V.A. Bavdekar, J. Prakash, S.C. Patwardhan, S.L. Shah, A moving window formulation for recursive Bayesian state estimation of systems with irregularly sampled and variable delays in measurements, Ind. Eng. Chem. Res. 53 (35) (2014) 13750–13763.
[30] F. Allgöwer, T.A. Badgwell, J.S. Qin, J.B. Rawlings, S.J. Wright, Nonlinear predictive control and moving horizon estimation – an introductory overview, in: Advances in Control, Springer, 1999, pp. 391–449.
[31] S. Shyamal, C.L.E. Swartz, A multi-rate moving horizon estimation framework for electric arc furnace operation, IFAC PapersOnLine 49 (7) (2016) 1175–1180.
[32] S. Shyamal, C.L.E. Swartz, Multi-rate moving horizon estimation for an electric arc furnace steelmaking process, in: AIChE Annual Meeting, San Francisco, 2016.
[33] M.M. Rashid, P. Mhaskar, C.L. Swartz, Multi-rate modeling and economic model predictive control of the electric arc furnace, J. Process Control 40 (2016) 50–61.
[34] Y. Li, R.J. Fruehan, Computational fluid-dynamics simulation of postcombustion in the electric-arc furnace, Metall. Mater. Trans. B 34 (3) (2003) 333–343.
[35] G.A. Irons, Developments in electric arc furnace steelmaking, in: AISTECH-Conference Proceedings, vol. 1, Association for Iron & Steel Technology, 2005, pp. 3.
[36] S. Matson, W.F. Ramirez, Optimal operation of an electric arc furnace, 57th Electric Furnace Conference (1999) 719–730.
[37] J.G. Bekker, I.K. Craig, P.C. Pistorius, Modeling and simulation of an electric arc furnace process, ISIJ Int. 39 (1) (1999) 23–32.
[38] A. Fathi, Y. Saboohi, I. Škrjanc, V. Logar, Comprehensive electric arc furnace model for simulation purposes and model-based control, Steel Res. Int. 88 (3) (2017) 1600083.
[39] R.D.M. MacRosty, C.L.E. Swartz, Dynamic modeling of an industrial electric arc furnace, Ind. Eng. Chem. Res. 44 (2005) 8067–8083.
[40] Process Systems Enterprise Ltd, gPROMS, 2015, 2015 www.psenterprise.com/gproms.
[41] Y. Ghobara, Modeling, Optimization and Estimation in Electric Arc Furnace (EAF) Operation (Master's thesis), McMaster University, 2013.
[42] J. Andersson, A General- Purpose Software Framework for Dynamic Optimization (PhD thesis), Arenberg Doctoral School, KU Leuven, Department of Electrical Engineering (ESAT/SCD) and Optimization in Engineering Center, Kasteelpark Arenberg 10, 3001- Heverlee, Belgium, 2013 October.
[43] Z.K. Nagy, R.D. Braatz, Robust nonlinear model predictive control of batch processes, AIChE J. 49 (7) (2003) 1776–1786.
[44] D.G. Robertson, J.H. Lee, On the use of constraints in least squares estimation and control, Automatica 38 (7) (2002) 1113–1123.
[45] C.V. Rao, J.B. Rawlings, D.Q. Mayne, Constrained state estimation for nonlinear discrete-time systems: stability and moving horizon approximations, IEEE Trans. Autom. Control 48 (2) (2003) 246–258.
[46] A. Alessandri, M. Baglietto, G. Battistelli, Moving- horizon state estimation for nonlinear discrete-time systems: new stability results and approximation schemes, Automatica 44 (7) (2008) 1753–1765.
[47] A. Küpper, M. Diehl, J.P. Schlöder, H.G. Bock, S. Engell, Efficient moving horizon state and parameter estimation for SMB processes, J. Process Control 19 (5) (2009) 785–802.
[48] V.M. Zavala, L.T. Biegler, Optimization-based strategies for the operation of low- density polyethylene tubular reactors: moving horizon estimation, Comput. Chem. Eng. 33 (1) (2009) 379–390.
[49] F. Magnusson, J. Åkesson, Dynamic optimization in JModelica.org, Processes 3 (2) (2015) 471–496.

Please cite this article in press as: S. Shyamal, C.L.E. Swartz, Real-time energy management for electric arc furnace operation, J. Process Control (2018), https://doi.org/10.1016/j.jprocont.2018.03.002

[50] R. López-Negrete, L.T. Biegler, A moving horizon estimator for processes with multi-rate measurements: a nonlinear programming sensitivity approach, J. Process Control 22 (4) (2012) 677–688.
[51] L. Ji, J.B. Rawlings, Application of MHE to large-scale nonlinear processes with delayed lab measurements, Comput. Chem. Eng. 80 (2015) 63–72.
[52] S. Kramer, R. Gesthuisen, S. Engell, Fixed structure multirate state estimation, in: American Control Conference (ACC), vol. 7, IEEE, 2005, pp. 4613–4618.
[53] S. Krämer, R. Gesthuisen, Multirate state estimation using moving horizon estimation, 16th IFAC World Congress, IFAC Proceedings, vol. 38 (1) (2005) 1–6.
[54] C.C. Qu, J. Hahn, Computation of arrival cost for moving horizon estimation via unscented Kalman filtering, J. Process Control 19 (2) (2009) 358–363.
[55] R. Lopez- Negrete, S.C. Patwardhan, L.T. Biegler, Constrained particle filter approach to approximate the arrival cost in moving horizon estimation, J. Process Control 21 (6) (2011) 909–919.
[56] J.B. Rawlings, Moving horizon estimation, Encycl. Syst. Control (2014) 1–7.
[57] R. Huang, V.M. Zavala, L.T. Biegler, Advanced step nonlinear model predictive control for air separation units, J. Process Control 19 (4) (2009) 678–685.
[58] P. Kühl, M. Diehl, T. Kraus, J.P. Schlöder, H.G. Bock, A real-time algorithm for moving horizon state and parameter estimation, Comput. Chem. Eng. 35 (1) (2011) 71–83.
[59] L.T. Biegler, Nonlinear Programming: Concepts, Algorithms, and Applications to Chemical Processes, SIAM, 2010.
[60] A. Wächter, L.T. Biegler, On the implementation of an interior-point filter line-search algorithm for large-scale nonlinear programming, Math. Progr. 106 (1) (2006) 25–57.
[61] A.C. Hindmarsh, P.N. Brown, K.E. Grant, S.L. Lee, R. Serban, D.E. Shumaker, C.S. Woodward, SUNDIALS: suite of nonlinear and differential/algebraic equation solvers, ACM Trans. Math. Softw. (TOMS) 31 (3) (2005) 363–396.

Please cite this article in press as: S. Shyamal, C.L.E. Swartz, Real-time energy management for electric arc furnace operation, J. Process Control (2018), https://doi.org/10.1016/j.jprocont.2018.03.002